Available online at www.sciencedirect.com
SCIENCE DIRECT®
Physica B 369 (2005) 261–265
PHYSICA B
www.elsevier.com/locate/physb

Magnetoresistance in $La_{2/3}Ca_{1/3}MnO_3/La_{2/3}Sr_{1/3}CoO_3$ bilayers

Jia-feng Feng[a], Kun Zhao[b,c,d,*], Yan-hong Huang[b], Song-qing Zhao[b], Hui-bin Lu[b], Jian-gao Zhao[a], Xiu-feng Han[a], Wen-shan Zhan[a], Hong-kuen Wong[e]

[a]*State Key Laboratory for Magnetism, Beijing National Laboratory for Condensed Matter Physics, Institute of Physics, Chinese Academy of Sciences, Beijing 100080, PR China*
[b]*Key Laboratory of Optical Physics, Beijing National Laboratory for Condensed Matter Physics, Institute of Physics, Chinese Academy of Sciences, Beijing 100080, PR China*
[c]*Spintronics Laboratory, School of Physics Science and Information Technology, Liaocheng University, 252059 Shandong Province, PR China*
[d]*International Center for Materials Physics, Chinese Academy of Sciences, Shenyang 110016, PR China*
[e]*Department of Physics, The Chinese University of Hong Kong, Shatin, Hong Kong, PR China*

Received 14 March 2005; received in revised form 22 August 2005; accepted 24 August 2005

Abstract

Perovskite $La_{2/3}Ca_{1/3}MnO_3$ (LCMO)/$La_{2/3}Sr_{1/3}CoO_3$ (LSCO) and LSCO/LCMO bilayer films have been fabricated on single-crystal $NdGaO_3$ substrates (1 1 0), and their transport and magnetic properties have been investigated. The magnetoresistance of the bilayer LSCO/LCMO is about 1.7% under the field of 10 kOe at 230 K, whereas that of the bilayer LCMO/LSCO is larger and is ~10%. A waist-like hysteresis loop occurs in LSCO/LCMO, while a single-step one in LCMO/LSCO. The behavior is explained by some magnetic coupling.

PACS: 75.47.GK; 75.47.Lx; 75.30.Et; 75.70.Ak

Keywords: Colossal magnetoresistance; Manganites; Magnetic coupling; Bilayer film

1. Introduction

The doped manganites, $RE_{1-x}A_xMnO_3$ (RE = rare-earth and A = alkaline-earth elements), have been the topic of intense scrutiny in recent years because of displaying a fascinating diversity of behavior including several forms of magnetic,

*Corresponding author. Group L03, Institute of Physics, Chinese Academy of Sciences, P.O.Box 603, Beijing 100080, PR China. Tel.: +86 10 82648060; fax: +86 10 82649451.
E-mail address: ainiphoto@163.com (K. Zhao).

0921-4526/$ - see front matter © 2005 Elsevier B.V. All rights reserved.
doi:10.1016/j.physb.2005.08.021

orbital and charge orderings as well as the colossal magnetoresistance (CMR) near the ferromagnetic Curie temperature (T_C) [1,2]. Another distinguishing feature is that the spin polarization in the doped manganites is believed to be 100% due to the half-metallic nature, where only the single spin band crosses the Fermi level [3]. Besides the scientific interest to investigate the elusive mechanism of CMR effect, some of attention has been focused on the technological applications of the doped manganites in spin-polarized tunnel junctions [4] as well as in spin-polarized current injection devices [5]. However, their contact with antiferromagnetic (AF) perovskite layers and substrates may give rise to some divertive effects, which may alter the magnetotransport properties of the devices, if the doped manganites serve as ferromagnetic layers (FM). The divertive effects are usually associated with lattice distortion, the dynamics of film growth or others. Therefore, to optimize extrinsic magnetoresistance (MR) effects in the doped manganite-based nanostructures, it would be necessary to have a knowledge of the divertive effects in the magnetic behavior and magnetotransport properties of the individual layers. In addition, because of the high spin polarization of conduction electrons in the doped manganites, spin-polarized tunnel junctions with the doped manganites as FMs show high low-field MR [6]. It is argued that the high MR originates from the inter-layer magnetic coupling, although a full understanding of the effects still remains little. In this paper, we have a systemic study of the magnetotransport properties of bilayer $La_{2/3}Ca_{1/3}MnO_3$ (LCMO)/$La_{2/3}Sr_{1/3}CoO_3$ (LSCO) which gives some interesting phenomena that may be introduced by lattice mismatch or other reasons.

2. Experiment procedures

LSCO (50 nm) /LCMO (50 nm) and LCMO (50 nm)/LSCO (50 nm) bilayers have been deposited on (1 1 0) $NdGaO_3$ (NGO) single-crystal substrates by the facing-target sputtering technique [7–10]. Ceramic LCMO and LSCO targets were sintered by standard procedure. The structure and orientation of the bilayers were studied by a Huber four-circle X-ray diffractometer using Cu Kα X-rays. The resistivity ρ as a function of temperature was measured by the standard four probe technique with CIP (current in plane) geometry and the distance between voltage contacts was fixed at 6 mm. The MR was examined with an applied magnetic field (H) of up to 10 kOe. The H was in the film plane and perpendicular to the current direction, which was also in the film plane. The MR ratios were estimated using the expression of $MR = [\rho\ (0)- \rho\ (H)]/\rho\ (0)$, where $\rho\ (H)$ and $\rho\ (0)$ are resistivities with the applied field H and without it, respectively. $\rho(0)$ was taken as the standard value because MR effects for LCMO/LSCO or LSCO/LCMO were not saturated with an applied field of up to 10 kOe. The magnetic moment of the samples as functions of temperature and magnetic field was measured by utilizing a vibrating sample magnetometer. During the measurements, a magnetic field was applied parallel to the film surface. A small nonhysteretic contribution from the NGO substrate was eliminated by separately measuring its diamagnetic response. Especially the behavior of bilayers at 230 K is described. This temperature is lower than T_{MI} (the metal–insulator transition temperature of LCMO layer) and higher than T_{MM} (the metal–metal transition temperature of LSCO layer). In our setup, there is a broad temperature range within which the LCMO ($T_{MI} \approx 240$ K) is ferromagnetic and metallic, whereas the LSCO ($T_{MM} \approx 210$ K) is paramagnetic and metallic.

3. Results and discussion

X-ray diffration (XRD) study shows that both as-prepared bilayers, LCMO (50 nm)/LSCO (50 nm)/NGO and LSCO (50 nm)/LCMO (50 nm)/NGO, are good epitaxial films, and only those peaks coherent with the substrate were detected as shown in Fig. 1. The peaks are much broader, and the reflections of Cu Kα_1 and Kα_2 cannot be distinguished from each other. For thin epitaxial film, the in-plane lattice of the sample has to match that of the substrate, and then the lattice expansion is essentially the expansion of the out-of-plane lattice parameter. LSCO has smaller lattice

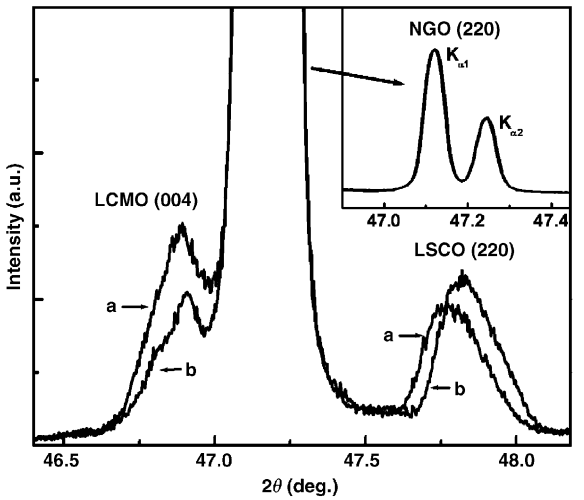

Fig. 1. X-ray diffraction patterns of (a) LSCO (50 nm)/LCMO (50 nm)/NGO and (b) LCMO (50 nm)/LSCO (50 nm)/NGO. The inset is a close view of the (220) peak of the NGO substrate.

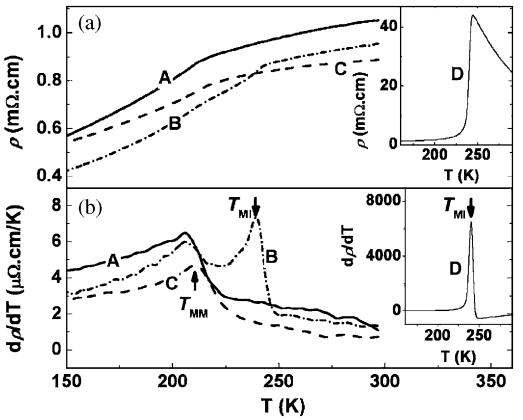

Fig. 2. (a) Resistivity (ρ) and (b) differential coefficient (dρ/dT) as functions of temperature for single layer and bilayer films. A, B, C, and D denote LCMO (50 nm)/LSCO (50 nm), LSCO (50 nm)/LCMO (50 nm), LSCO (100 nm), and LCMO (100 nm) films, respectively.

parameters than that of LCMO, whereas NGO exhibits similar lattice constants with LCMO. A tensile strain in LSCO/NGO and LSCO/LCMO and a negligibly small lattice strain in LCMO/NGO should be expected. Therefore, the out-of plane lattice of LSCO and LCMO layer should be stress and expansion, respectively. It is clear that the peak position of the LSCO for LCMO/LSCO/NGO is different from that for LSCO/LCMO/NGO, and the diffraction peaks of the LCMO layers almost are at the same position for the two bilayers. This means that the LSCO layer in LCMO/LSCO/NGO is compressed much more between upper LCMO layer and the substrate NGO, than that in LSCO/LCMO/NGO. This kind of lattice distortion may cause the different magnetotransport properties between LSCO/LCMO and LCMO/LSCO bilayers.

Fig. 2(a) and (b) show the temperature dependence of the resistivity (ρ) and its temperature coefficient (dρ/dT) of samples. The curves of LCMO (100 nm)/NGO and LSCO (100 nm)/NGO are also shown in Fig. 2 for comparison. The LSCO (50 nm)/LCMO (50 nm) and LCMO (50 nm)/LSCO (50 nm) are metallic, and the resistivity increases with temperature until ~210 K. At ~210 K, which is no different from the T_{MM} of LSCO (100 nm) film (see the curve C), the peak value of dρ/dT occurs arising from the metal–metal transition of the LSCO layer. This kind of transition was also observed in bulk LSCO, and was ascribed to the change of magnetic order [11]. A significant change with the increase of temperature has been observed when the LSCO is the upper layer. At ~240 K another metal–metal transition occurs for the LSCO/LCMO bilayer different from that for the LCMO/LSCO bilayer. In fact, compared with the T_{MI} of LCMO (100 nm) film (the cross point in dρ/dT ~ T), this transition is resulted from the metal–insulator transition of LCMO layers. So we also denote the temperature as T_{MI}.

The MR ratios of bilayers LSCO (50 nm)/LCMO (50 nm) and LCMO (50 nm)/LSCO (50 nm) at ~230 K are presented in Fig. 3. For LSCO/LCMO, the MR ratio is about 1.7% at $H = 10$ kOe. However, the MR, ~10% of LCMO/LSCO, is much higher than that of LSCO/LCMO. Although both bilayers have equal thicknesses, the LSCO in LCMO/LSCO is compressed much more than that in LSCO/LCMO. It may bring larger lattice distortion, and then bring new magnetic interactions between LSMO and LCMO, which make the MR ratio of LCMO/LSCO is much

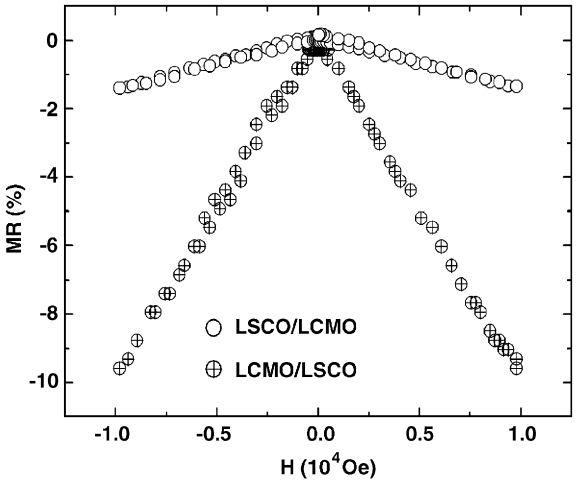

Fig. 3. MR of LCMO (50 nm)/LSCO (50 nm) and LSCO (50 nm)/LCMO (50 nm) bilayers measured at 230 K.

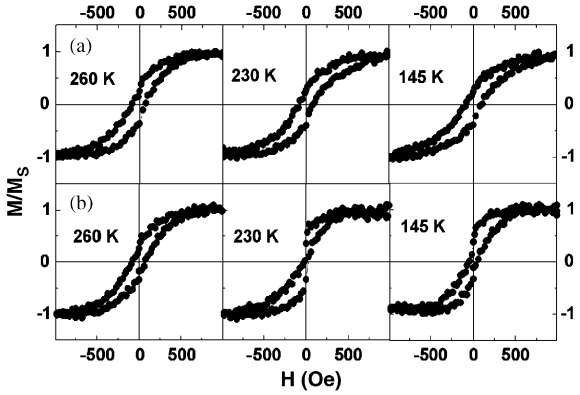

Fig. 4. Magnetic hysteresis loops varying with the temperature of (a) LCMO (50 nm)/LSCO (50 nm) and (b) LSCO (50 nm)/LCMO (50 nm).

higher. The detailed explanation may be obtained from the hysteresis loops as follows.

Fig. 4 shows the hysteresis of LCMO (50 nm)/LSCO (50 nm) and LSCO (50 nm)/LCMO (50 nm) at different temperatures. No marked changing is observed and all the loops are smooth for LCMO/LSCO. However, an obvious change of the loops for LSCO/LCMO occurs between 140 K and 240 K and a narrow waist is found, which may imply the difference in magnetization behavior and

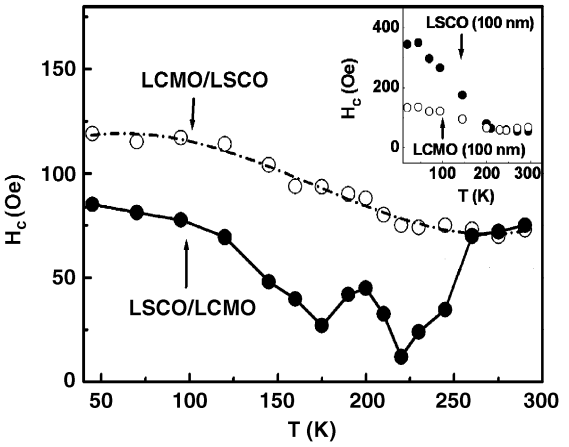

Fig. 5. H_C as a function of temperature for LCMO (50 nm)/LSCO (50 nm), LSCO (50 nm)/LCMO (50 nm), LSCO (100 nm), and LCMO (100 nm) films, respectively.

the role of the inter-layer magnetic coupling between LCMO and LSCO [12].

Fig. 5 is a summary of magnetic coercivity H_C against the temperature. As for LCMO and LSCO single layer films, their coercivities are distinct obviously in the temperature range between 140 and 250 K (see the inset of the Fig. 5). Arising from the different coercivities between LCMO and LSCO layers, a two-step loop should have been measured if the systems were decoupled. In contrast, for LCMO/LSCO, single-step magnetization loop appears and the H_C basically reduces monotonously with increasing the temperature, indicating that there is a ferromagnetic coupling in the bilayer. Furthermore, the H_C of LSCO/LCMO varies irregularly between 140 and 240 K corresponding to the waist-like hysterisis loops in Fig. 4(b). Especially, the value is lower than that of LCMO and LSCO single layer films in this temperature range. It is quite reasonable that the exchange coupling between ferromagnetic LCMO layers and unferromagnetic LSCO layer brings on the nonmonotonic H_C and narrow waist-like loops for LSCO/LCMO bilayer. The peak value of H_C at 200 K roots in the paramagnetic–ferromagnetic transition of LSCO layer. The different trends of H_C between the two bilayers suggest that different coupling modes rule over, which may be resulted from the different lattice distortion. It is argued

that these results originate from the inter-layer magnetic interaction, although a full understanding of the effects still remains open.

4. Conclusion

In summary, the perovskite LCMO/LSCO and LSCO/LCMO bilayers are fabricated by a facing-target sputtering technique. The MR ratio of the bilayer LSCO/LCMO is about 1.7% under a field of 10 kOe at 230 K, whereas that of the bilayer LCMO/LSCO is larger and is ~10%. The waist-like hysteresis of LSCO/LCMO and single-step loop of LCMO/LSCO indicates that some exchange magnetic couplings exist in the systems.

Acknowledgements

This work has been supported by the National Natural Science Foundation of China (Nos. 50371102 and 10334070), the National Key Basic Research and Development Program of China (No. 2004CB619004), the Research Foundation of Shandong Provincial Education Department of China (No. 03A05), and China Postdoctoral Science Foundation.

References

[1] R. Von Helmolt, J. Wecker, B. Holzapfel, L. Schultz, K. Samwer, Phys. Rev. Lett. 71 (1993) 2331.
[2] S. Jin, T.H. Tiefel, M. McCormack, R.A. Fastnacht, R. Ramesh, L.H. Chen, Science 264 (1994) 413.
[3] J.-H. Park, E. Vescovo, H.-J. Kim, C. Kwon, R. Ramesh, T. Venkatesan, Nature (London) 392 (1998) 794.
[4] C.N.R. Rao, Philos. Trans. R. Soc. London Ser A: Math. Phys. Sci. 256 (1998) 23.
[5] C. Zener, Phys. Rev. 81 (1951) 440.
[6] T. Obata, T. Manako, Y. Shimakawa, Y. Kubo, Appl. Phys. Lett. 74 (1999) 290.
[7] K. Zhao, H.K. Wong, Physica B 349 (2004) 238.
[8] K. Zhao, L. Zhang, H. Li, H.K. Wong, J. Appl. Phys. 95 (2004) 7363.
[9] K. Zhao, L.Z. Zhou, C.H. Leung, C.F. Yeung, C.K. Fung, H.K. Wong, J. Cryst. Growth 237–239 (2002) 608.
[10] K. Zhao, H.K. Wong, J. Cryst. Growth 256 (2003) 283.
[11] M. Itoh, I. Natori, S. Kubota, K. Motoya, J. Phys. Soc. Japan 63 (1994) 1486.
[12] J.-M. Liu, Q. Huang, J. Li, C.K. Ong, Z.G. Liu, Appl. Phys. A 69 (Suppl.) (1999) S663.